International Journal of Design & Nature and Ecodynamics
Vol. 20, No. 6, June, 2025, pp. 1387-1396
Journal homepage: http://iieta.org/journals/ijdne

Novel Imidazole Derivative AOMI: Enhanced Antibacterial/Anti-Biofilm Properties and Mechanistic Insights

Hamsa S. Aidi*, Khalida F. Al-Azawi, Buthenia A. Hasoon

Applied Science Department, University of Technology, Baghdad 10011, Iraq

Corresponding Author Email: as.22.91@grad.uotechnology.edu.iq

https://doi.org/10.18280/ijdne.200619

Received: 9 May 2025
Revised: 19 June 2025
Accepted: 24 June 2025
Available online: 30 June 2025

Keywords:
Schiff base, imidazole, antibacterial, antioxidant, docking studies

ABSTRACT

The research delves into the creation and assessment of an innovative imidazole derivative, AOMI, which shows remarkable antibacterial and anti-biofilm capabilities. The synthesis and evaluation of 2-(2-(anthracen-9-yl)-5-oxoimidazolidin-1-yl)-1-methyl-1H-imidazol-4(5H)-one (AOMI), a new imidazole derivative with strong antibacterial and anti-biofilm capabilities, are investigated in this study using molecular docking experiments. AOMI was created by reacting anthracene-9-carbaldehyde with creatinine to obtain the Schiff base (E)-2-(anthracen-9-ylmethyleneamino)-1-methyl-1H-imidazol-4(5H)-one (AMMI). The use of techniques like FTIR, ^{1}H NMR, and ^{13}C NMR allowed for the confirmation of the produced compounds' structures. The antibacterial tests showed that AOMI was highly effective against S. aureus and E. coli when mixed with amoxicillin, with inhibition zones as large as 22.25 ± 0.30 mm. It should be noted that AOMI outperformed amoxicillin in terms of anti-biofilm activity and had a minimum inhibitory concentration (MIC) of 200 Δg/mL. Furthermore, DPPH experiments demonstrated that AOMI exhibited antioxidant activity, with scavenging rates reaching a maximum of 79.10% at the dose that was tested. According to the molecular docking data, there were strong contacts with the target protein's active site residues through electrostatic and hydrogen bonding interactions, as evidenced by a binding energy of -30.5897 kcal/mol and an RMSD value of 2.4709 Å. We need to learn more about how AOMI works and make more imidazole derivatives since these results suggest that it could be a very good way to treat bacterial infections.

1. INTRODUCTION

The medicinal chemistry community has taken note of imidazole derivatives since they can do a lot of different things in the body, such as fighting viruses, fungi, and bacteria. Because antibiotic resistance is becoming more common, we need new compounds that can effectively target resistant bacterial strains right away. Schiff bases have shown promise as antibacterial agents because they can affect microbial cell membranes and DNA, stopping important biological processes [1, 2]. When primary amines and carbonyl compounds are mixed together, they make Schiff bases. We don't know much about how these compounds work, but they seem to focus on interactions between DNA and bacterial membranes.

The German chemist Hugo Schiff described Schiff bases in 1864 as chemicals bearing a hydrocarbyl group on the nitrogen atom. These compounds are commonly known as (imines) azomethines (C=N-) [1]. By virtue of steric and electronic properties, aldehydes react more rapidly than ketones in these condensation reactions [2]. Pharmacological advancements in the last several years have expanded well beyond the realm of predicted bioactive drug production. In their quest to find and create novel, diverse molecules with a wide range of chemical structures, researchers have encountered many obstacles. Compounds with a Schiff base have medicinal potential and are used to treat a range of illnesses [3]. Analgesic, antimalarial, anti-inflammatory, anti-proliferative, antiviral, antipyretic, antifungal, and antibacterial are only a few of the many biological effects demonstrated by Schiff bases, which appear to be dependent on the presence of an imine group [4]. On the other hand, the need for more effective chemicals is prompted by the rising level of bacterial resistance. Medicinal uses have been found for heterocyclic compounds with five-member rings; imidazole derivatives are one such chemical. Researchers in the medical sector are motivated to synthesize a significant number of novel imidazole-based compounds due to the comprehensive therapeutic qualities of imidazole derivative medications [5]. Antibacterial, anti-inflammatory, antioxidant, anticancer, and antifungal are just a few of the many uses for imidazole in medicine. Imidazole appears in two tautomeric forms because the hydrogen atom can be positioned on either of the two nitrogen atoms. It is a five-membered ring compound that is soluble in water and polar solvents. It is worth mentioning that there is ongoing research and development in imidazole synthesis and functionalization at various positions to improve its action.

In addition to its potential antibacterial activities, the 5B6N protein—also known as peroxidase 6—is essential for cellular protection against oxidative stress. Bacterial infections can

produce reactive oxygen species (ROS), which can be detoxified by their enzymatic activity. Molecular docking tests have indicated that AOMI can attach to the active site of peroxidase 6. This might make its antibacterial actions greater by modifying how bacteria respond to oxidative stress [6, 7]. This study uses the anthracene ring structure to generate a new imidazole derivative called 2-(2-(anthracen-9-yl)-5-oxoimidazolidin-1-yl)-1-methyl-1H-imidazol-4(5H)-one (AOMI) [8]. It is known that imidazole derivatives can kill bacteria, but the anthracene portion was chosen because it can make this action greater by helping the chemical pass past membranes and connect with DNA [9]. Adding aromatic structures to imidazole derivatives can change how they work in the body by making them more lipophilic and helping them bind to cellular targets more easily [10]. Scientists are looking at a lot of imidazole derivatives as possible new drugs, which is quite exciting [11]. For the first time, scientists have studied a new structure of 2-(2-sub-5-oxo-imidazolidin-1 yl)-1-methyl-1,5-dihydro-4H-imidazol-4-one (AOMI) and Schiff base (AMMI). They used several ways to make it. Scientists are studying the synthesis, characterization, and biological evaluation of AOMI as part of a larger effort to find a means to manufacture antibacterial treatments that work against resistant strains [12, 13]. We will also run molecular docking tests to see how AOMI attaches to the 5B6N protein, which may protect cells from oxidative stress and fight bacteria [6, 11]. We believe that studying these processes can help us create new medical imidazole compounds. The purpose of this study was to determine the best C2-C6 candidate by looking at their shape (FTIR, ^{1}HNMR, and ^{13}CNMR), how well they combat bacteria, and how well they fight *E. coli* and *S. aureus* bacteria in silico.

2. EXPERIMENTAL

2.1 Materials and methods

The ethanol for the Schiff base production was provided by Alpha Chemika, while the other starting chemicals were acquired from Fluka and Sigma-Aldrich. The melting points of all the produced compounds are measured using a heated capillary tube. The functional groups in all of them are validated using KBr discs and FTIR spectroscopy with the SHIMADAZU FTIR Spectroscopy (IR Affinity-1) from the BPC-Analysis Center. It was necessary to plot FTIR, C^{13}, and HNMR spectra in order to examine these substances. After being collected from the wounds of sick patients, the chemicals were tested for their antibacterial characteristics [14, 15]. This helped validate their composition. They were tested in the docking program once their effectiveness was proven, and the one that proved to be the most beneficial was chosen as a possible treatment.

2.2 Synthesis of Schiff base (AMMI)

A mixture of 0.113 g of creatinine and 0.001 mol of anthracene-9-carbaldehyde in 30 ml of ethanol and a few drops of glacial acetic acid (G.A.A.) was used to create Schiff bases (AMMI) [16]. The combination was refluxed for ten hours. The product was recrystallized from 100% ethanol after the solvent was exhausted [17].

2.3 Synthesis of 2-(2-sub-5-oxo-imidazolidin-1-yl)-1-methyl-1,5-dihydro-4H-imidazol-4-one (AOMI)

After refluxing for 20 hours with a few drops of DMF, a solution containing 0.001 mol of Schiff base and 0.07 g of a-amino acetic acid in 25 ml of ethanol was recrystallized from absolute ethanol.

2.4 Pathogenic bacterial identification

Staphylococcus aureus and *Escherichia coli* isolates were collected from the microbiology lab and used for bacterial identification [18]. The VITEK-2 compact system was used to correctly identify the microbiological isolates at the species level [19]. For *S. aureus*, the Gram-positive (GP) card was utilized, and for *E. coli*, the Gram-negative (GN) card was employed.

2.5 Anti-bacterial analyze

To measure the efficacy against bacteria, the agar well diffusion method was employed. Mueller-Hinton agar was used as the growth medium, and it was produced as directed by the manufacturer [20, 21]. After adjusting the overnight bacterial culture to a 0.5 McFarland standard for turbidity, a sterile swab was used to evenly streak 0.1 mL of the culture onto the agar surface [22]. The next step was to create four wells in the agar using a sterile cork borer with a diameter of 6 mm [23]. The component AOMI was added to each well in 0.1 mL increments at concentrations of 200, 400, 600, and 800 µg/mL using a sterile micropipette. A well containing just distilled water served as a negative control. All studies were conducted in triplicate [24, 25]. After incubation at 37°C for 24 hours, the inhibition zones of the antibacterial activity were measured in millimeters. To enhance the antimicrobial test, positive controls were utilized. Amoxicillin was used to suppress the bacterial strains *Staphylococcus aureus* and *Escherichia coli*. To get the right concentrations, stock solutions of the control microbes were made and diluted in a serial fashion. Results from these created imide compounds were compared to these established positive controls in order to assess their relative antibacterial activity [26].

2.6 Anti-biofilm test

To test AOMI's ability to prevent biofilm formation, crystal violet (C.V.) staining was employed. At 200, 400, 600, and 800 µg/mL, the biofilm inhibitory concentrations were ascertained using the microtiter plate technique. Following treatment, the wells were cleaned, and 0.1% C.V. was added to each. After incubating for 15 minutes, the plates were washed and the dye was removed. A measurement of the biofilm's quantity was made by dissolving the bound dye in 95% ethanol and then taking the optical density (OD) at 595 nm [16, 22].

2.7 Preparation of 1,1-Diphenyl-2-picryl-hydrazyl (DPPH) solution

In a volumetric flask, a solution was prepared by thawing 0.002g of DPPH in 100 mL of 100% methanol. Then, to prevent photo-oxidation, cover with aluminum foil and shake vigorously using a vortex. The detection of antioxidant efficacy is facilitated by this solution [27].

2.8 Antioxidant activity

The antioxidant properties of AOMI were evaluated using the DPPH test. When dissolved in 100 mL of 100% methanol, 0.002 g of DPPH forms a light-protected solution. Mixed with 490 µL of AOMI at various doses (200, 400, 600, and 800 µg/mL), the DPPH solution was exposed to light. The ascorbic acid positive control used a concentration of 100 µg/mL. A control solution was prepared using 500 µL of DPPH in order to facilitate comparison. Following 30 minutes of incubation at room temperature, a measurement of 517 nm was recorded. We repeated each measurement three times to guarantee precise and trustworthy findings. An equation was given for the purpose of determining the antioxidant activity [24].

2.9 Molecular docking

When the correct docking parameters are employed to study interactions between various docking sites and ligand scores, the 5B6N code can reflect protein structures associated with antioxidant and antibacterial characteristics. To protect cells from oxidative stress and free radicals, proteins such as this one are crucial. In crystal structures of sulfinic acid-bound human peroxiredoxin 6, the 5B6N codes are linked to protein active site 1 [28]. The crystal structure, which has a resolution of 2.90 Å and is considered appropriate for docking research, was obtained from the protein data bank site (https://www.rcsb.org/structure/5B6N). A typical ideal RMSD score is approximately 2 Å, corresponding to an energy level of -7 Kcal/mol or below. These two numbers are often used to check the accuracy of a molecular docking result. We have successfully docked the optimized modified selenium papain molecule (Se-Papain) onto the 1 receptor active site. The majority of the time for the docking and scoring calculations, a program named Molecular Operating Environment (MOE, 2022) was utilized. By intentionally leaving solvent molecules (water) in active site 1 when designing the receptor protein, the MOE software ensured that a hydrogen bond would form between the ligand and the target. Protonation followed by X-ray diffraction-based structural correction of the protein. This optimization was carried out using Amber 10's energy refinement and supported model construction, which harnesses the power of the Extended Hückel Theory (EHT) [29].

2.10 Statistical analysis

The data was statistically analyzed with the help of GraphPad Prism 6. To compare things, we used an unpaired t-test. The results from three separate tests are shown as the average plus or minus the standard deviation (SD) [18, 19].

3. RESULTS AND DISCUSSION

3.1 Chemistry

Schiff base [C2] can be synthesized by reacting creatinine and anthracene-9-carbaldehyde with ethyl alcohol and a few drops of glacial acetic acid, as indicated in Figure 1. The combination of Schiff base and α-amino acetic acid produces imidazole molecules. Infrared, carbon-13, and hydrogen one nuclear magnetic resonance spectra were used to identify each of the chemicals that were successfully synthesized.

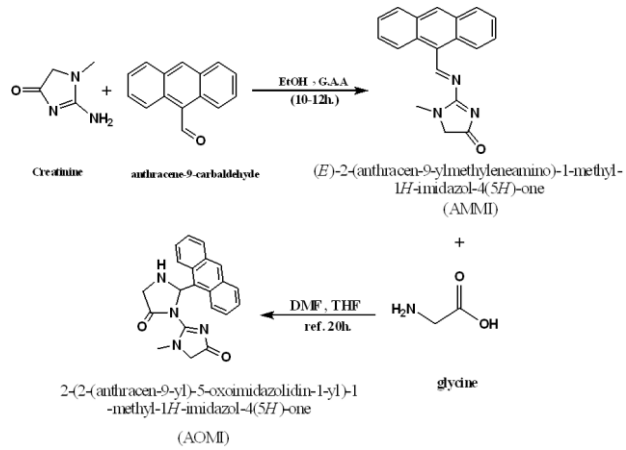

Figure 1. Synthesis of AOMI compound

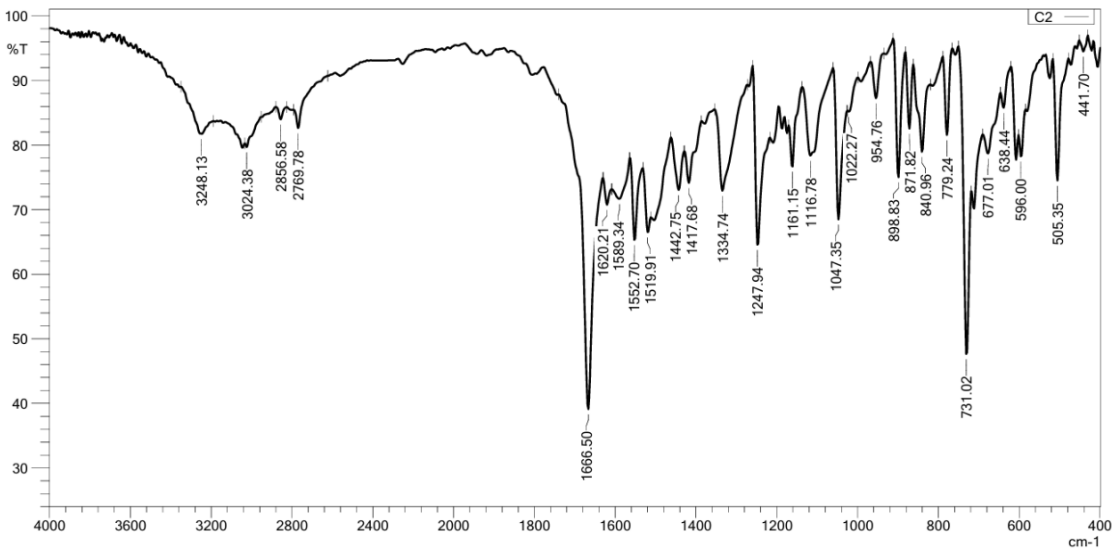

Figure 2. FTIR of compound (AMMI)

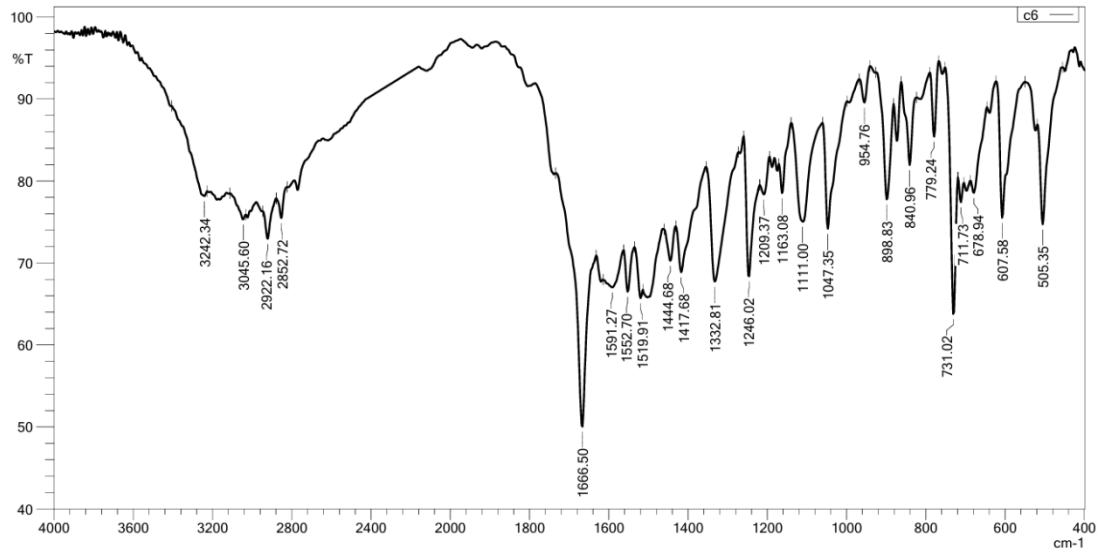

Figure 3. FTIR of compound (AOMI)

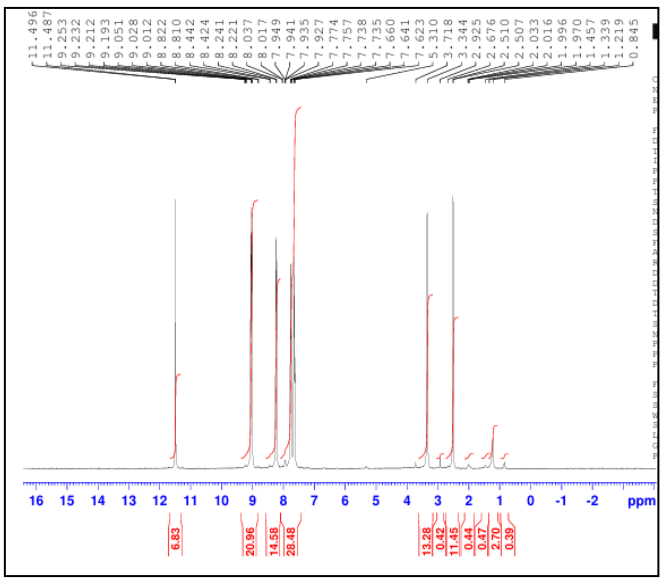

Figure 4. H1NMR of compound AMMI

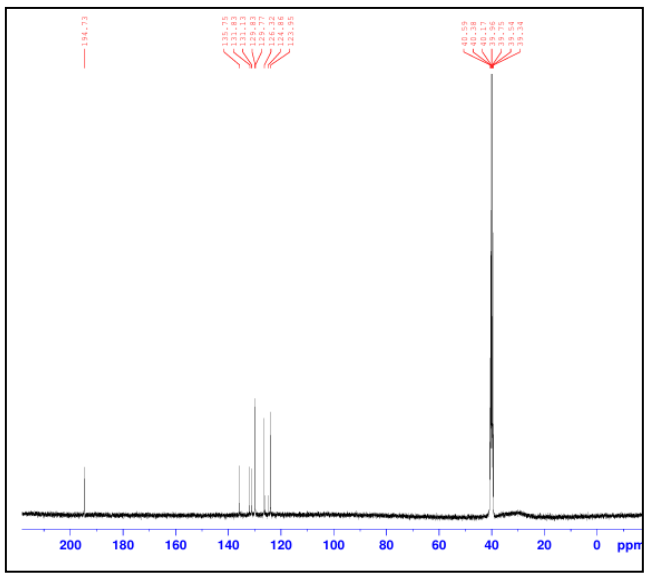

Figure 6. The C^{13} spectroscopy of AMMI

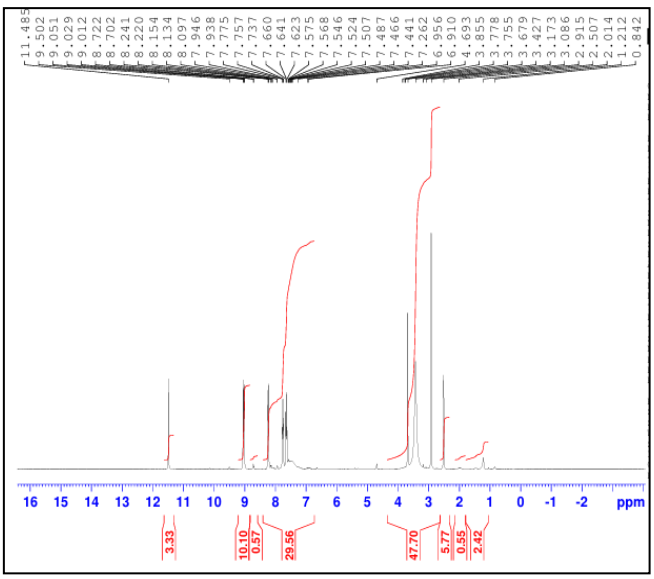

Figure 5. H1NMR of compound AOMI

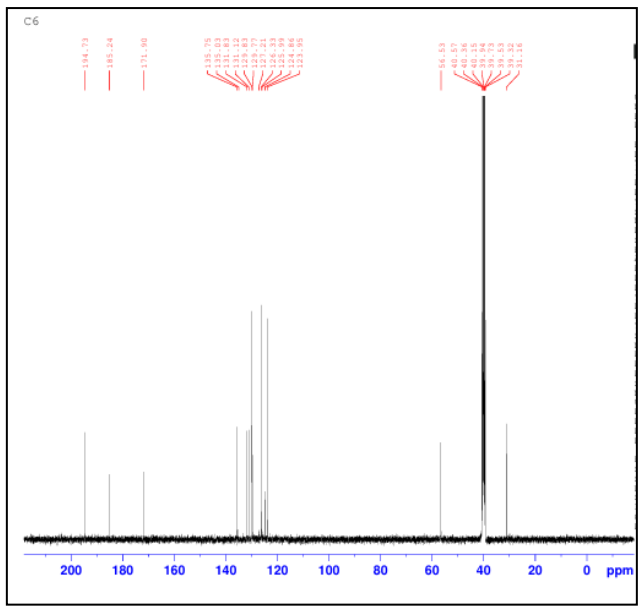

Figure 7. The C^{13} spectroscopy of (AOMI)

Table 1. Physical properties and FT-IR spectral data cm^{-1} of synthesized compounds (AMMI and AOMI)

				Major FT-IR Absorption cm^{-1}				
Comp.	m.p.℃	Color	Yield%	*v*(C-H) arom.	*v*(C=N), *v*(C-N)	*v*(C=O) cyclic amide	*v*(C-H) aliph.	*v*(C=C) arom
AMMI	98-100	Yellow	60%	3024.38	1620.21, 1334.74	1666.50	2856.68, 2769.78	1589.34, 1552.70, 1519.91
AOMI	232-235	Orange	75%	3045.60	1620.21, 1332.81	1666.50	2922.16, 2852.72	1591.27, 1552.70, 1519.91

3.2 Characterization

The KBr pellet method was used to record the FT.IR spectra of the Schiff base (AMMI) and the imidazole compound (AOMI). Due to the presence of carbon-hydrogen bond vibrations at specified cm^{-1}, cm^{-1}, and cm^{-1} values in Schiff bases (AMMI), the band for v(NH_2) has disappeared. The absorption bands at (3242.34) cm^{-1}, (3045.60) cm^{-1}, (2922.16, 2852.72) cm^{-1}, (1666.50) cm^{-1}, (1620.21) cm^{-1}, and (1591.27, 1552.70, 1519.91) cm^{-1} correspond to the v(N-H), v(C-H) arom, v(C-H) aliphatic, v(C=O) cyclic amide, v(C=N), and v(C=C) aromatic, respectively, as seen in the FT-IR spectra of the (AOMI) compound. These bands are shown, among others, in Table 1 and Figures 2 and 3.

Figure 3 represents the FTIR of compound (AOMI), and Figure 4 represents the H1NMR of compound (AMMI). Also, Figure 5 shows the H1NMR of compound (AOMI). Figure 6 expresses the C^{13} spectroscopy of (AMMI), and Figure 7 expresses the C^{13} spectroscopy of (AOMI). In addition, Table 2 expresses the ^{1}HNMR spectral data of AMMI-AOMI, and Table 3 expresses the C^{13} NMR spectral data for (AMMI-AOMI).

Table 2. ^{1}HNMR spectral data of AMMI-AOMI

Component	^{1}HNMR Signals Data, d (ppm)
AMMI	δ 2.67(s,3H,N-CH_3), δ 3.34(s,2H,CH_2-C=O), δ 7.62 - 8.03(m,6H,Ar-H.), δ 8.42 (s,1H,N=CH-Ar) of Schiff bases, δ 8.81 (s,1H,Ar-H)
AOMI	δ 3.08ppm(s,3H,CH_3-N), δ 3.42ppm (s 3H,CH_2(C=O)NH), δ 4.69ppm (s,2H, CH_2(C=O)NR), δ 6.9ppm(1H,-CH-Ar), δ 7.26-7.77 ppm (m,5H,Arom.) and δ 8.19 ppm (s, 1H, NH-CH_2)

Table 3. C^{13} NMR spectral data for AMMI-AOMI

Component	C^{13} NMR Signals Data, d (ppm)
AMMI	δ 194.73 (C=N), δ 123.95-135.75 (Aromatic Carbons), δ 39.34-40.59 (CH_3 in an aliphatic environment)
AOMI	δ 194.73 (C=O-N), δ131.12-135.75(Carom., Anthracene), δ 185.24(C=O), δ171.90 (C=N) group

3.3 Anti-bacterial activity

The well diffusion method was performed to find out how well AOMI kills *E. coli* and *S. aureus* bacteria. We looked at four different diluted concentrations of AOMI (200, 400, 600, and 800 μgmL^{-1}) to examine how they affected the growth of bacteria. Figure 8 illustrates the areas where the bacteria can't grow. Panel (a) shows the impacts on *E. coli*, and panel (b) shows the effects on *S. aureus*. The data is shown as the mean plus or minus the standard deviation, and the inhibition rates for each level of AOMI are listed. For *E. coli*, the inhibition rates at different concentrations of (AOMI) were 15.06 mm, 16.73 mm, 17.20 mm, and 18.06 mm, in that order. The inhibition zone for *S. aureus* got bigger as the concentration of AOMI went up. The rates were 16.40 mm, 17.43 mm, 18.20 mm, and 19.05 mm, in that order. Changes to the bacterial cell membrane [11-13] could be one reason why the antibiotic action works. AOMI creates reactive oxygen species (ROS), which are harmful to cells and destroy their membranes [14, 15]. The size and concentration of AOMI impact how well it kills germs. It can also make membranes more flexible and put osmotic stress on them.

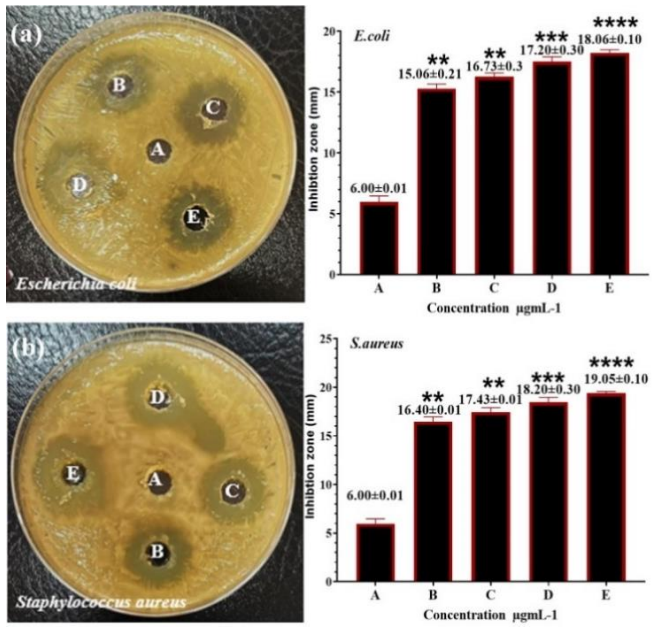

Figure 8. (a) When tested against *E. coli*, AOMI showed antibacterial activity; (b) *S. aureus* (A, B, C, and D were tested with different pore sizes)

A is shown with a control pore size of 6 mm, C, with a pore size of 400 μgmL^{-1}, and D, with a pore size of 600 μgmL^{-1}. For B, it represents the *S. aureus* A, B, C, and D were tested with different pore sizes. Eight hundred micrograms of Ethanol are utilized. It shows the mean plus or minus the standard deviation of the data from three separate studies. * $p \leq 0.01$, ** $p \leq 0.001$, and $p \leq 0.05$

The size of AOMI's particles has a huge effect on how successfully it kills germs. This is because it changes how well it can get past bacterial membranes and into cells. Because they have a bigger surface area-to-volume ratio, smaller particles normally pass through membranes more easily. This helps them engage with lipid bilayers and absorb the active substance more easily. Also, smaller particles may be able to enter through the holes in bacterial cell walls more easily, which means they can build up higher concentrations at the target site and kill more bacteria. They might also have stronger effects on membrane parts, which could make the membrane less stable and more permeable, which could cause the cell to burst. Also, making the particles bigger can make

the synergistic effects of AOMI stronger when it is used with other antibacterial therapies. This might help get beyond resistive obstacles. So, future research should focus on figuring out the size range of AOMI's particles and how it affects how they interact with membranes. This will help us understand how it operates and how it could be utilized as a treatment [1]. The anthracene ring structure of AOMI makes it simpler for π-π stacking interactions to develop, which makes it much better at killing bacteria. These interactions let the chemical cling better to bacterial membranes, which helps it go through and break apart lipid bilayers. Also, π-π stacking helps AOMI stay stable overall, which means it can work when it interacts with target sites. This keeps its antibacterial actions going. These interactions also make AOMI more lipophilic, which means it can build up in bacterial cells and work better. To make AOMI (10) operate better as an antibacterial drug, it is critically crucial to understand how π-π stacking works.

3.4 Anti-biofilm action

The effectiveness of AOMI in killing bacteria and inhibiting biofilm formation was examined in this study using strains of Staphylococcus aureus and Escherichia coli. The bacteria that were studied for their biofilm-forming abilities were examined using a crystal violet (C.V.) dye with a concentration of 0.1%. When tested against *E. coli* and *S. aureus*, AOMI proved to be a highly effective germ killer.

C_6 is highly effective in inhibiting biofilm development, according to the data. The MIC, or minimum inhibitory concentration, was 200 µg/mL, the lowest effective concentration of C_6. Based on these findings, AOMI may be a valuable compound for inhibiting the development of microbial biofilms. Compared to the untreated control strains, *E. coli* and *Staphylococcus aureus* bacteria that underwent AOMI therapy exhibited less clustering and adhesion. The anti-bacterial qualities of AOMI were demonstrated when it was tested to prevent the formation of biofilms using crystal violet staining. Based on this estimation, AOMI has the potential to be an effective method for preventing biofilm formation. Compared to the untreated controls, bacterial cultures treated with AOMI deposited less biofilm and had a simpler biofilm structure [16-18]. Figure 9 shows the inhibition of biofilm formation by AOMI against *E. coli.* and *S. aureus*.

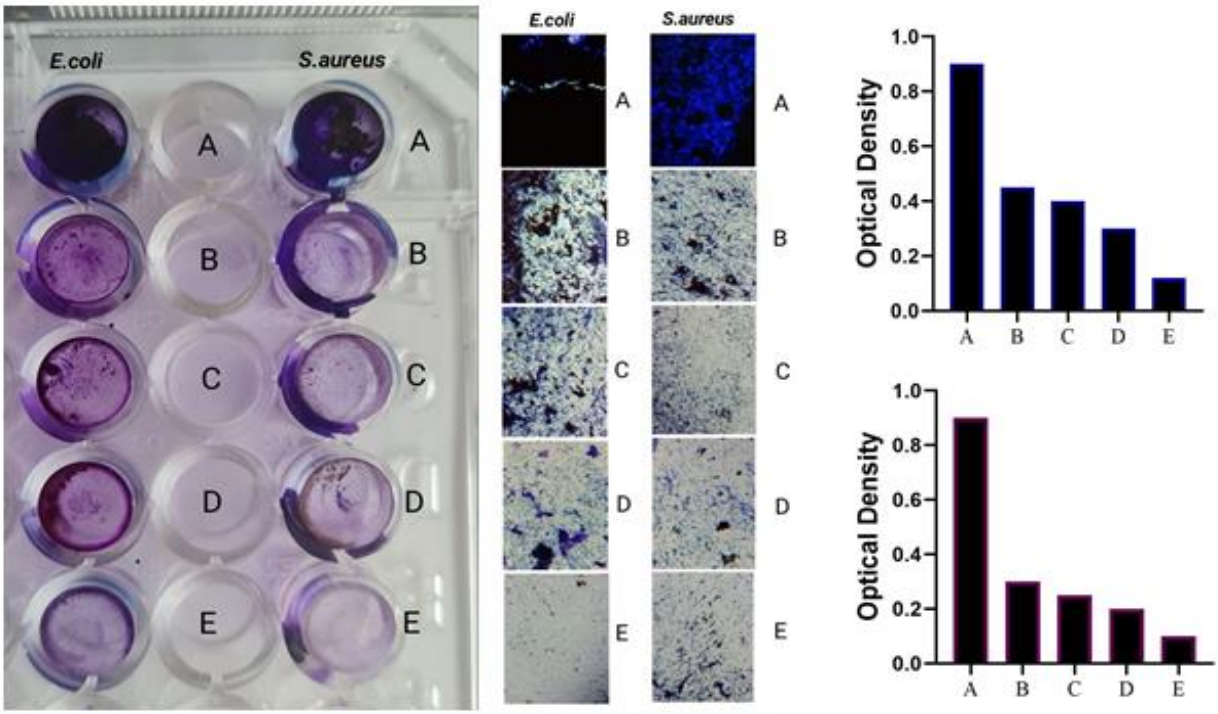

Figure 9. Inhibition of biofilm formation by AOMI against *E. coli.* and *S. aureus*
A (control D.W), B (200 µgmL^{-1}), C (400 µgmL^{-1}), D (600 µgmL^{-1}), and E (800 µgmL^{-1})

Table 4. Action of antimicrobial agents on *S. aureus* and *Escherichia coli* (AOMI)

Pathogein	Mean ± (AOMI)	Standard (AOMI) + Antibiotic	Deviation Antibiotic	(mm) Negative D.W Control	P-value
E.coli	15.06 ± 0.12a	20.73 ± 0.10c	19.73 ± 0.10 ^{b}	6.00±0.5	0.000
S. aureus	17.06 ± 0.12a	22.25 ± 0.30 ^{d}	21.25 ± 0.30 ^{b}	6.00±0.5	0.000

Note that values that have the same letter repeatedly are not statistically significant, whereas values that have distinct letters show a substantial difference.

3.5 Synergistic effect

Table 4 shows the results of the antimicrobial tests that were done on all of the isolates that were examined. Amoxicillin alone formed an inhibitory zone of 15.06 ± 0.12 mm for *E. coli* isolates and 17.06 ± 0.12 mm for S. aureus. When given alone

with AOMI, the inhibitory zone for *S. aureus* grew to 20.73 ± 0.10 mm. When given with amoxicillin and AOMI, it grew to 22.25 ± 0.30 mm. Adding amoxicillin to the mix of AOMI and *E. coli* made the inhibitory zone grow from 19.73 ± 0.10 mm to 21.25 ± 0.30 mm. The control inhibitory zone was 6.10 ± 0.10 mm bigger than the experimental settings, which means that the bacterial cell walls were highly damaged, causing the cells to break down. It is thought that the combined effects of amoxicillin and AOMI, which stop topoisomerase IV and DNA gyrase from working, kill bacterial cells. Incorporating AOMI into antibiotic regimens allows us to decrease dosage, mitigate toxicity, and impede the development of antibiotic-resistant microorganisms. Because it is a synthetic chemical with unique properties, these findings suggest that AOMI may be an effective treatment for bacterial infections. Because it is biocompatible and has low toxicity to cells, AOMI has numerous potential applications in industry and biology. By demonstrating how simple it is to prepare, this study clarifies why the amoxicillin (AOMI) combination is effective against Gram-positive bacteria. The presence of hydrophilic glycoproteins, in particular, weakened the bacterial cell walls when they came into contact with the combined chemicals. This issue allowed the AOMI to bypass the Gram-positive bacteria with relative ease. The antibiotic also increased the membrane's permeability, which facilitated the absorption of (AOMI). Final analysis: AOMI's coordinated action resulted in bacterial cell death by increasing lipid peroxidation and producing reactive oxygen species (ROS). All of the above-mentioned procedures point to AOMI's promise as a remedy for antibiotic resistance and persistent biofilms that cause bacterial diseases. The molecular processes and interactions that make AOMI effective in combo therapy should continue to be investigated in future studies. Examine the cited works [19, 20].

3.6 Antioxidant evaluation

Researchers evaluated AOMI's free radical scavenging capabilities using the DPPH assay. Its scavenging activity was 20% at 400 µg/mL, 47.36% at 600 µg/mL, 71.10% at 600 µg/mL, and 79.50% at 800 µg/mL.

The scavenging activity peaked at 79.10% at 800 µg/mL. With an antioxidant activity of 800 µg/mL, ascorbic acid—a well-liked positive control—is able to effectively combat free radicals. The capacity of AOMI to combat free radicals, however, remained much reduced [21]. The free radical DPPH gives organic solvents their characteristic deep violet hue and stays put for long periods of time. A well-known and easy way to determine something's antioxidant effectiveness is the DPPH test. This assay measures the ability of various compounds to neutralize free radicals, providing insight into their antioxidant capabilities [22]. An antioxidant has the ability to transform the DPPH radical from a dark purple color to a colorless or light yellow substance, which is the fundamental assumption of the DPPH test. The degree of discolouration clearly impacts the substance's antioxidant capabilities. This test is a fantastic way to rapidly evaluate the effectiveness of many different items in fighting free radicals [23] because it is both effective and easy to execute. Electric currents are the basis of the experiment. The interaction between stable free radicals and antioxidants, which releases electrons, causes the DPPH solution to change color [24]. Yes, this proves it to be accurate. An excellent way to determine whether compounds are safe to use is to test their effectiveness against free radicals. The scavenging capacity of AOMI is, unsurprisingly, inferior to that of ascorbic acid, even when administered in higher doses.

3.7 Molecular docking results

With the right docking parameters, the 5B6N code generates a protein structure that interacts with different docking sites and ligand scores; this structure has anti-bacterial and anti-oxidant properties.

To protect cells from oxidative stress and free radicals, proteins such as this one are crucial. Crystal structures of sulfonic acid-bound human peroxiredoxin 6 show 5B6N codes linked to the protein active site 1 [1]. The crystal structure, which has a resolution of 2.90 Å and is considered adequate for docking research, was obtained from the protein data bank site (https://www.rcsb.org/structure/5B6N) [2]. With an energy level of -7 Kcal/mol or lower, the optimal RMSD score is frequently near 2 Å. These two numbers are often used to check the accuracy of a molecular docking result. Here at receptor active site 1, we have docked the most abundant molecule optimized for selenium, papain, and se-papain. For the docking and scoring calculations, a program named MOE was utilized. By intentionally leaving solvent molecules (water) in active site 1 when designing the receptor protein, the MOE software ensured that a hydrogen bond would form between the ligand and the target. Protonation followed by X-ray diffraction-based structural correction of the protein. The following optimization takes advantage of EHT's motivating feature, Amber 10's energy refinement, and assisted model creation [3].

3.8 Molecular docking for antioxidant and antibacterial

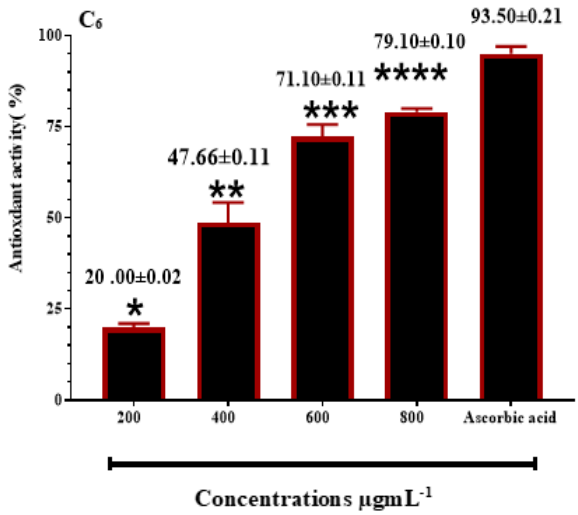

Figure 10. Antioxidant activity of AOMI

The molecular docking investigation of 5B6N revealed significant interactions with residues in the active site, which enhances its binding affinity and suggests potential biological activity. The binding mechanisms significantly stabilize the ligand-receptor complex through the use of hydrogen bond acceptors and pi-cation interactions. The interaction analysis of the binding affinity of the AOMI-5B6N complex, which is -5.5623 kcal/mol, revealed an RMSD of 2.4709 Å. Significant interactions with SER 75 (A) (OG) at 3.05 Å and ARG 41 (A) (NH2) at 3.15 Å are seen in the H-bond acceptors,

respectively. The reference [4] stated that at 4.12 Å, 4.68 Å, and 4.03 Å, respectively, there are phosphorylated interactions with ARG 106 (A) (NE, NE) and LYS 125 (A) (CD). The AOMI-5B6N complex improves binding affinity and stability via strong hydrogen bonding and pi-cation interactions with key active site residues (ARG, SER, and LYS). The overall binding energy of the complex is -30.5897 kcal/mol. The rather strong ligand-protein interactions demonstrated by the total binding energy values of -33.04 kcal/mol indicate the possibility of functional activity. Antibacterial and antioxidant bioactive chemicals often employ a high-affinity binding mechanism [5]. This is further supported by the fact that it interacts with ARG 106 and LYS 125 multiple pi-cation times (Figures 10, 11, and Table 5). Table 5 represents the Molecular docking results of the (AOMI) complex with the 5B6N Receptor. The Abbreviations are the following: H-acc = Hydrogen acceptor; π-cat = Pi–cation interaction; π–H = Pi-hydrogen interaction; 6R = Aromatic six-membered ring. The compound Name is AOMI, which refers to the tested ligand compound docked with the target protein 5B6N.

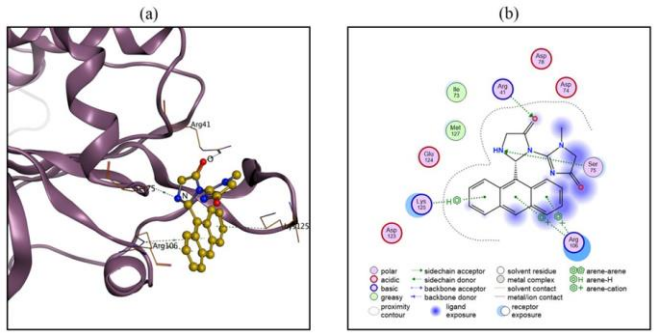

Figure 11. 3D and 2D representation of (AOMI) interaction with a binding site in 5B6N protein

Table 5. Molecular docking results of (AOMI), complex with 5B6N Receptor

Score	RMSD	Residue	Interaction	Type	d (Å)	E
-5.56	2.47	SER75 (A)	N–OG	H-acc	3.05	-1.42
		ARG41 (A)	O–NH_2	H-acc	3.15	-1.44
		ARG106 (A)	6R–NE	π-cat	4.12	-1.12
		ARG106 (A)	6R–NE	π-cat	4.68	-1.08
		LYS125 (A)	6R–CD	π–H	4.03	-0.65
						Total E: -33.04

4. CONCLUSIONS

A novel imidazole derivative, AOMI, has been synthesized. The features were confirmed using FTIR, ^{1}H NMR, and ^{13}C NMR. The antibacterial activities of AOMI were shown to be strong when tested against Staphylococcus aureus and Escherichia coli. Upon addition of amoxicillin, a maximal inhibition zone of 22.25 ± 0.30 mm was achieved. A minimum inhibitory concentration (MIC) of 200 µg/mL was observed for AOMI. At MIC, AOMI demonstrated strong anti-biofilm activity, leading to a significant reduction in biofilm production. At 800 µg/mL, AOMI showed antioxidant activity with scavenging rates reaching a high of 79.10%. Molecular docking experiments indicate that the binding energy of the target protein (5B6N) is -30.5897 kcal/mol. Interactions with active site residues were discovered to be successful, suggesting potential mechanisms for antioxidant and antibacterial activity. The mechanisms of AOMI warrant further investigation because of its promise as a therapy for bacterial infections.

ACKNOWLEDGMENT

This research was supported by internal funding from the Department of Applied Sciences, University of Technology, Iraq.

REFERENCES

[1] Raczuk, E., Dmochowska, B., Samaszko-Fiertek, J., Madaj, J. (2022). Different Schiff bases—Structure, importance and classification. Molecules, 27(3): 787. https://doi.org/10.3390/molecules27030787

[2] Aulakh, J.S., Kumar, V., Kim, K.H. (2019). A review of the applications of Schiff bases as optical chemical sensors. Trends in Analytical Chemistry, 116: 74-91. https://doi.org/10.1016/j.trac.2019.04.025

[3] Ashraf, T., Ali, B., Qayyum, H., Haroone, M.S., Shabbir, G. (2023). Pharmacological aspects of schiff base metal complexes: A critical review. Inorganic Chemistry Communications, 150: 110449. https://doi.org/10.1016/j.inoche.2023.110449

[4] Ceramella, J., Iacopetta, D., Catalano, A., Cirillo, F., Lappano, R., Sinicropi, M.S. (2022). A review on the antimicrobial activity of Schiff bases: Data collection and recent studies. Antibiotics, 11(2): 191.

[5] Slassi, S., Aarjane, M., Yamni, K., Amine, A. (2019). Synthesis, crystal structure, DFT calculations, Hirshfeld surfaces, and antibacterial activities of Schiff base based on imidazole. Journal of Molecular Structure, 1197: 547-554. https://doi.org/10.1016/j.molstruc.2019.07.071

[6] Zheng, X., Ma, Z., Zhang, D. (2020). Synthesis of imidazole-based medicinal molecules utilizing the van leusen imidazole synthesis. Pharmaceuticals, 13(3): 37. https://doi.org/10.3390/ph13030037

[7] Bettencourt, A.P., Castro, M., Silva, J.P., Fernandes, F., Coutinho, O.P., Sousa, M.J., Proença, M.F., Areias, F.M. (2019). Phenolic imidazole derivatives with dual antioxidant/antifungal activity: Synthesis and structure-activity relationship. Medicinal Chemistry, 15(4): 341-351. https://doi.org/10.2174/1573406414666181005143431

[8] Sharma, P., LaRosa, C., Antwi, J., Govindarajan, R., Werbovetz, K.A. (2021). Imidazoles as potential anticancer agents: An update on recent studies. Molecules, 26(14): 4213. https://doi.org/10.3390/molecules26144213

[9] Işık, A., Acar Çevik, U., Sağlık, B.N., Özkay, Y. (2019). Synthesis, characterization, and molecular docking study of some novel imidazole derivatives as potential antifungal agents. Journal of Heterocyclic Chemistry, 56(1): 142-152. https://doi.org/10.1002/jhet.3388

[10] Hossain, M., Nanda, A.K. (2018). A review on heterocyclic: Synthesis and their application in medicinal chemistry of imidazole moiety. Science Journal of Chemistry, 6(5): 83-94. https://doi.org/10.11648/j.sjc.20180605.12

[11] Al-Majedy, Y.K., Ibraheem, H.H., Issa, A.A., Jabir, M.S., Hasoon, B.A., Al-Shmgani, H.S., Sulaiman, G.M. (2023). Synthesis, biomedical activities, and molecular docking study of novel chromone derivatives. Journal of Molecular Structure, 1295(1): 136647. https://doi.org/10.1016/j.molstruc.2023.136647

[12] Abed, H.H., Al-Azawi, K.F., Majeed, I.Y., Hasoon, B.A. (2025). Synthesis and evaluation of chalcone derivatives for antimicrobial and antioxidant activities using microwave-assisted methodology. AIP Conference Proceedings, 3169(1): 020006. https://doi.org/10.1063/5.0255186

[13] El Sayed, D.S., Hassan, S.S., Jassim, L.S., Issa, A.A., Al-Oqaili, F., Albayaty, M.K., Hasoon, B.A., Jabir, M.S., Rasool, K.H., Elbadawy, H.A. (2025). Structural and topological analysis of thiosemicarbazone-based metal complexes: Computational and experimental study of bacterial biofilm inhibition and antioxidant activity. BMC Chemistry, 19(1): 24. https://doi.org/10.1186/s13065-024-01338-5

[14] Al-Azawi, K.F., Hasoon, B.A., Ismail, R.A., Rasool, K.H., Jabir, M.S., Shaker, S.S., Jawad, K.H., Abdula, A.M., Ghotekar, S., Swelum, A.A. (2025). Pharmaceutical properties of novel 3-((diisopropylamino)methyl)-5-(4-((4-(dimethylamino)benzylidene)imino)phenyl)-1,3,4-oxadiazole-2(3H)-thione. Scientific Reports, 15: 15019. https://doi.org/10.1038/s41598-025-98061-5

[15] Hussein, H.H., Al-Azawi, K.F., Hasoon, B.A., El-Sayed, D.S. (2024). Advance screening of bis-azetidinone derivatives: Synthesis, spectroscopy, antioxidant and antimicrobial analysis with molecular docking assessment. Current Organic Synthesis, 22(3): 396-409. https://doi.org/10.2174/0115701794318870240923073910

[16] Mahmood, T.M., Jawad, K.H., Jabir, M.S. (2025). Synergistic effect of AgNPs and gentamicin: Inhibition of multi-drug resistance bacterial biofilm formation and down-regulated fimH gene. Nano-Structures & Nano-Objects, 41: 101437. https://doi.org/10.1016/j.nanoso.2025.101437

[17] Sheltagh, E.R., Almukhtar, O., Rafeeq, M.F., Rasool, K.H., Mahdi, S.A., Jawad, K.H., Hasoon, B.A., Issa, A.A., Jabir, M.S., Jawad, S.F. (2024). Synthesis, pharmaceutical properties, and in silico study of ZnO@TiO_2 nanocomposite. Inorganic Chemistry Communications, 169: 112994. https://doi.org/10.1016/j.inoche.2024.112994

[18] Hussein, N.N., Al-Azawi, K., Sulaiman, G.M., Albukhaty, S., et al. (2023). Silver-cored ziziphus spina-christi extract-loaded antimicrobial nanosuspension: Overcoming multidrug resistance. Nanomedicine, 18(25): 1839-1854. https://doi.org/10.2217/nnm-2023-0185

[19] Yosif, H.M., Hasoon, B.A., Jabir, M.S. (2024). Laser ablation for synthesis of hydroxyapatite and Au NP conjugated cefuroxime: Evaluation of their effects on the biofilm formation of multidrug resistance Klebsiella pneumoniae. Plasmonics, 19(3): 1085-1099. https://doi.org/10.1007/s11468-023-02053-y

[20] Hasan, D.M.A., Hasoon, B.A., Abdulwahab, A.I., Jawad, K.H. (2022). Biological activities of ethanolic extract produced by Cucurbita pepo plant. Revista Bionatura, 7(2): 19. https://doi.org/10.21931/RB/2022.07.02.19

[21] Hasoon, B.A., Jawad, K.H., Mohammed, I.S., Hussein, N.N., Al-Azawi, K.F., Jabir, M.S. (2024). Silver nanoparticles conjugated amoxicillin: A promising nano-suspension for overcoming multidrug resistance bacteria and preservation of endotracheal tube. Inorganic Chemistry Communications, 165: 112456. https://doi.org/10.1016/j.inoche.2024.112456

[22] Al-Azawi, K.F., Hussein, N.N., Al Majeed, R.M.A. (2022). Evaluation of the antimicrobial and antioxidant activities of the Ziziphus spina-christi plant leaves. AIP Conference Proceedings, 2437(1): 020082. https://doi.org/10.1063/5.0092320

[23] Hameed, A.H., Mohamed, E.A., Sami, R.H., Hasoon, B.A., Al-Azawi, K.F., Alawsi, N.G.K., Nasser, S.M. (2024). Investigating the effect of alcoholic extract as antimicrobial, antioxidant, and anticancer drug biosynthesized from onion Allium plant. Journal of Babol University of Medical Sciences, 26(1). https://doi.org/10.22088/jbums.26.1.37

[24] Jawad, K.H., Hasoon, B.A., Ismail, R.A., Shaker, S.S. (2022). Preparation of copper oxide nanosheets by pulsed laser ablation in liquid for anticancer, antioxidant, and antibacterial activities. Journal of the Indian Chemical Society, 99(11): 100773. https://doi.org/10.1016/j.jics.2022.100773

[25] Mahdi, L.H., Hasoon, B.A., Sulaiman, G.M., Mohammed, H.A., Jawad, K.H., Al-Dulimi, A.G., Essa, R.H., Albukhaty, S., Khan, R. (2024). Anti-microbial efficacy of L-glutaminase (EC 3.5.1.2) against multidrug-resistant Pseudomonas aeruginosa infection. The Journal of Antibiotics, 77(2): 111-119. https://doi.org/10.1038/s41429-023-00678-z

[26] Ahmed, M.E., Sulaiman, G.M., Hasoon, B.A., Khan, R.A., Mohammed, H.A. (2024). Green synthesis and characterization of apple peel-derived selenium nanoparticles for anti-fungal activity and effects of MexA gene expression on efflux pumps in Acinetobacter baumannii. Applied Organometallic Chemistry, 39(2): e7805. https://doi.org/10.1002/aoc.7805

[27] Hasoon, A.H., Hasoon, B.A., Mahmood, B.S., Mohamed, E.A., Jabir, M.S., Jawad, K.H., Hussein, N.N., Sulaiman, G.M., Dewir, Y.H., Mendler-Drienyovszki, N. (2024). Tangerine fruit peel extract mediated biogenic synthesized silver nanoparticles and their potential antimicrobial, antioxidant, and cytotoxic assessments. Green Processing and Synthesis, 13(1): 20240126.

[28] Jawad, K.H., Hasen, T.S., Hammoud, D., Hasoon, B.A., Jabir, M.S., Ghotekar, S., Swelum, A.A. (2025). Eco-friendly methods for synthesis of MgS@CuS nanocomposite for overcoming multidrug resistance bacteria: In silico assessment study. Journal of Drug Delivery Science and Technology, 109: 106998. https://doi.org/10.1016/j.jddst.2025.106998

[29] Najm, M.A.A., Shakir, H.A., Hasen, S.T., Jawad, K.H., Hasoon, B.A., Jabir, M.S., Molla, M.H. (2025). Titanium dioxide nanoparticles augment ciprofloxacin activity via inhibition of biofilm formation for multidrug resistance bacteria in-vitro and in silico prediction study. Scientific Reports, 15(1): 18014. https://doi.org/10.1038/s41598-025-93569-2